LONG-TERM TRENDS AND PROBABILITY DISTRIBUTION FUNCTIONS OF AIR POLLUTANT CONCENTRATIONS IN THE MEGACITY OF SÃO PAULO

Matheus Soares DÁRIO
Denise Gomes NOVAIS
Theotonio PAULIQUEVIS
Luciana Varanda RIZZO

ABSTRACT

Air quality conditions in many urban areas have improved in the last decades as a consequence of air pollution control policies and regulations. Mitigation strategies have been successful in reducing the concentration of primary pollutants like inhalable particulate matter (PM_{10}), but the control of secondary pollutants like tropospheric ozone (O_3) is still challenging in megacities like the Metropolitan Area of São Paulo (MASP) in Brazil. To support the development of effective mitigation strategies, it is crucial to characterize the statistical behavior of air pollutant concentrations and its long-term evolution. Probability Density Functions (PDF) can be useful to model site-specific air quality conditions, providing estimates for the frequency of extreme pollution events and exceedance of air quality standards. The current study aims to characterize which PDF model better fits and characterizes the variability of PM_{10} and O_3 concentrations in the MASP. For that, daily maximum moving average concentrations were analyzed between 2000 and 2023, characterizing the long-term trends and the frequency of exceedance of air quality standards. PM_{10} concentrations followed a lognormal PDF, with an expected value of 31 ± 15 $\mu g.m^{-3}$. O_3 followed a Gamma PDF, with an expected value of 68 ± 25 $\mu g.m^{-3}$. A consistent long-term decrease was observed for PM_{10} (-1.04 ± 0.09 $\mu g.m^{-3}.yr^{-1}$), while O_3 showed an increasing trend of 0.51 ± 0.04 $\mu g.m^{-3}.yr^{-1}$ in the summer. In recent years (2021-2023), the probability of exceedance of the World Health Organization guideline was 17.4 and 11.0%, respectively, for PM_{10} and O_3. In 2020, a statistically significant increase in O_3 expected values was observed, possibly associated with changes in the emission patterns of precursors due to the mobility restrictions imposed by the COVID-19 pandemic.

Keywords: Air quality; Particulate matter; Tropospheric ozone; São Paulo; Lognormal probability distribution; Gamma probability distribution.

RESUMO

POLUIÇÃO DO AR NA MEGACIDADE DE SÃO PAULO: TENDÊNCIA DE LONGO PRAZO E FUNÇÃO DISTRIBUIÇÃO DE PROBABILIDADE. A qualidade do ar tem melhorado em muitas cidades do mundo, devido a políticas de controle de emissão de poluentes atmosféricos. Estratégias de mitigação têm sido bem sucedidas para reduzir a concentração de poluentes primários como o material particulado inalável (MP_{10}), mas o controle de poluentes secundários como o ozônio (O_3) continua sendo um desafio em megacidades como a região metropolitana de São Paulo (RMSP), no Brasil. Para desenvolver estratégias efetivas de mitigação, é fundamental caracterizar estatisticamente as concentrações de poluentes e sua evolução temporal. Funções de densidade de probabilidade (PDF) são úteis para representar a variabilidade das condições de qualidade do ar, fornecendo estimativas para a probabilidade de ocorrência de episódios extremos de poluição do ar e de ultrapassagem de padrões. Este trabalho tem por objetivo caracterizar as distribuições de concentração de MP_{10} e O_3 na RMSP. Para

isso, dados de máxima diária da média móvel de concentração foram analisados entre 2000 e 2023, caracterizando tendências de longo prazo e a frequência de ultrapassagem de padrões de qualidade do ar. As concentrações de MP_{10} seguiram uma PDF lognormal com valor esperado de 31 ± 15 $\mu g.m^{-3}$. Já as concentrações de O_3 foram descritas por uma distribuição Gamma, com valor esperado de 68 ± 25 $\mu g.m^{-3}$. Uma tendência consistente de diminuição foi observada para o MP_{10} (-1,04 ± 0,09 $\mu g.m^{-3}.ano^{-1}$), enquanto o O_3 mostrou uma tendência de aumento de 0,51 ± 0,04 $\mu g.m^{-3}.ano^{-1}$ no verão. Nos últimos anos (2021-2023), a probabilidade de ultrapassagem dos padrões da Organização Mundial da Saúde foi de 17,4 e 11,0%, respectivamente para MP_{10} e O_3. Em 2020, foi observado um aumento estatisticamente significativo nos valores esperados de O_3, possivelmente associado com mudanças no padrão de emissão de precursores devido a restrições impostas no início da pandemia de COVID-19.

Palavras-chave: Qualidade do ar; Material particulado; Ozônio troposférico; São Paulo; Distribuição lognormal de probabilidade; Distribuição gamma de probabilidade.

1 INTRODUCTION

Air pollution is one of the main environmental problems in the Metropolitan Area of Sao Paulo (MASP), where a population of 21 million people is frequently exposed to inhalable particulate matter (PM_{10}) and ozone (O_3) concentrations above the air quality standards, with recognized impacts to the human health (ABE & MIRAGLIA 2016, GOUVEIA & JUNGER 2018, TAKANO et al. 2019). Although air quality has improved at MASP since the 1990s, as a consequence of successful regulations on emission sources (CARVALHO et al. 2015, ANDRADE et al. 2017, MARTINS et al. 2017), the control of secondary pollutants like O_3 is still a challenge (SCHUCH et al. 2019).

Vehicular emission is currently the main source of pollutants in the MASP, responding to 40% of PM_{10} emissions and 60% of nitrogen oxide (NOx) emissions (PÉREZ-MARTÍNEZ et al. 2017, CETESB 2023), the latter being a precursor to the photochemical production of tropospheric O_3. The light-duty vehicle fleet in the MASP uses fuel blends containing 27 to 95% of anhydrous ethanol, influencing the atmospheric chemistry and the partitioning of secondary pollutant precursors in a unique way (NOGUEIRA et al. 2014, SALVO & GEIGER 2014, BRITO et al. 2018, DOMINUTTI et al. 2020). Secondary particulate matter typically comprises 25% of PM_{10} in the MASP (CETESB 2023).

In addition to the dynamics and relevance of emission sources, the concentration of air pollutants depends on meteorological conditions. Periods of increased atmospheric stability and drought, typically observed during the austral winter in the MASP, hinder the dispersion of PM_{10} and other pollutants, leading to events of air quality standard exceedance (SANTOS et al. 2018, OLIVEIRA et al. 2022). In turn, the production of secondary pollutants like O_3 relies both on radiation input and on the emission strength and variety of precursors, so exposure to high concentrations of O_3 is a concern in the MASP during austral spring and summer (MARTINS et al. 2017, SCHUCH et al. 2019).

As such, the concentration of air pollutants is a consequence of a variety of processes acting simultaneously, including emissions, chemical and physical atmospheric processes, dispersion, and removal. Probability Density Functions (PDF) of pollutant concentration can be a useful tool to model site-specific air quality conditions, giving support for the development of strategies to control and mitigate this environmental problem. The distribution of air pollutant concentration is usually right-skewed so that low concentrations are more frequent, and extreme events of high concentrations form a long tail to the right. In the literature, many types of PDFs have been used to describe the statistical behavior of PM_{10} concentrations in urban environments, including lognormal, Weibull, Gamma, and Pearson V distributions (MIJIĆ et al. 2009, PAPANASTASIOU & MELAS 2010, CREMASCO et al. 2019, PLOCOSTE et al. 2020, MISHRA et al. 2021). The statistical behavior of O_3, in turn, is underrepresented in the recent literature (SHARMA et al. 2016). The best model to represent the PDF of air pollutants is site-specific and depends on local characteristics like proximity to emission sources, climate, and topography.

This study work aims to characterize the statistical behavior of PM_{10} and O_3 concentrations in the MASP between 2000 and 2023, assessing long-term trends and the frequency of exceedance of different air quality standards. In addition, changes in air quality conditions will be evaluated in the atypical year of 2020, when mobility restrictions during the COVID-19 pandemic affected air pollution emissions. The results can support the development of effective air pollution mitigation strategies for the MASP.

2 METHODS

2.1 Data

The Environmental Company of the State of São Paulo (CETESB) makes available the hourly concentration data of PM_{10} and O_3 at several monitoring stations in the MASP. Ten monitoring stations were selected for this study (Figure 1 and Table 1), considering data availability and spatial representativity above 100 m. The selected stations had a data coverage greater than 95% between 2000 and 2023. The monitoring stations sit at distances in the range of 5-22 km from each other, subject to very similar weather conditions. All of them are influenced by vehicular emissions to some extent, and industrial emissions also affect some of the stations (Table 1). Figure S1 in the Supplementary Material show that the concentration ranges were similar between the selected monitoring stations, especially in the case of O_3. The average time series of PM_{10} and O_3 concentrations were used to represent the mean air quality conditions in the MASP.

The hourly data was reduced to a daily basis, calculating the daily maximum of the 24h moving average (DMMA24) for PM_{10} and the daily maximum of the 8h moving average (DMMA8) for O_3. This metric was chosen to comply with the World Health Organization guidelines (WHO 2021) so that the statistics can be directly compared against air quality standards. In epidemiological studies, the health effects of short-term exposure to air pollution are typically assessed in time scales in the order of days (*e.g.*, CAI et al. 2016). Exceedance days are the ones in which the DMMA concentration exceeds the air quality standard. Table 2 shows a comparison between the current Brazilian National Air Quality

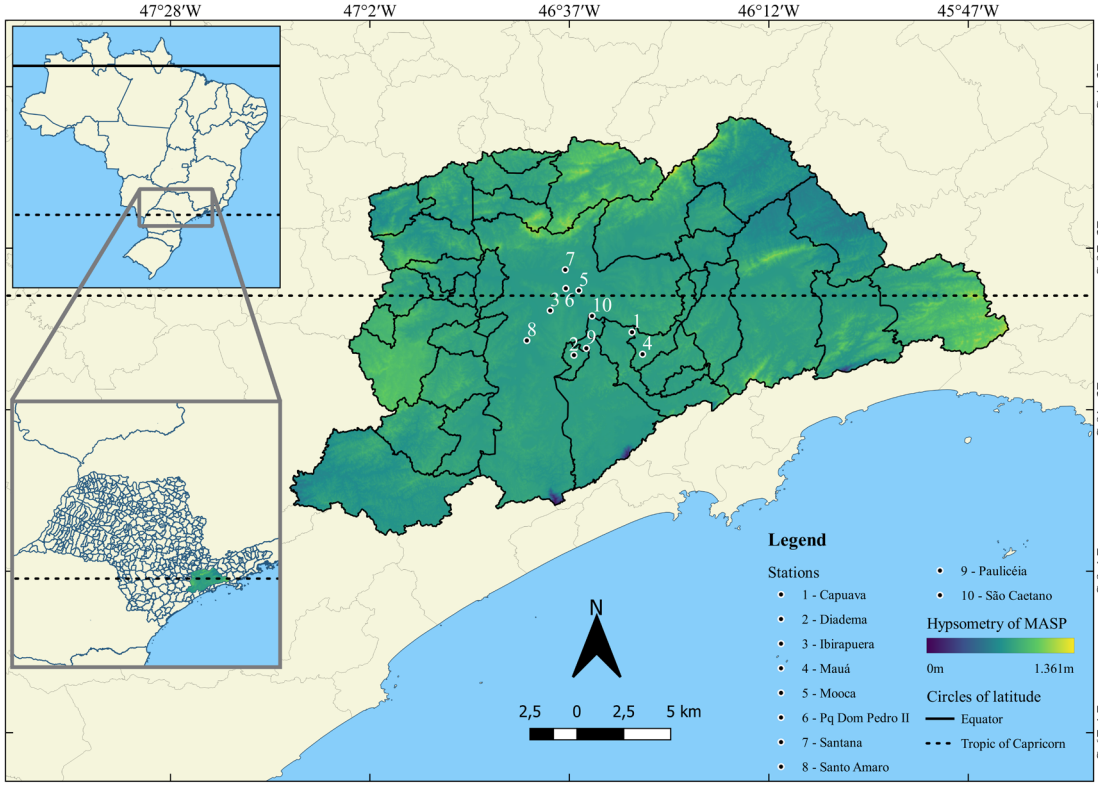

FIGURE 1 – Location of selected air quality stations and hypsometry of the MASP, based on data provided by DATAGEO, 2013.

TABLE 1 – Characteristics of selected air quality monitoring stations at the MASP (CETESB 2016).

	Stations	*Air pollutants*	*Spatial representativity*	*Air pollution sources*
1	Capuava	PM_{10}, O_3	501-4000 meters	Vehicles and Industrial
2	Diadema	PM_{10}, O_3	501-4000 meters	Vehicles
3	Ibirapuera	O_3	>4000 meters	Vehicles
4	Mauá	PM_{10}	501-4000 meters	Vehicles and Industrial
5	Mooca	O_3	501-4000 meters	Vehicles
6	Pq. D. Pedro II	PM_{10}, O_3	501-4000 meters	Vehicles
7	Santana	O_3	101-500 meters	Vehicles
8	Santo Amaro	PM_{10}	101-500 meters	Vehicles
9	Paulicéia	PM_{10}	501-4000 meters	Vehicles and Industrial
10	São Caetano	PM_{10}, O_3	101-500 meters	Vehicles and Industrial

TABLE 2 – Air quality standards for PM_{10} and O_3, as defined by the World Health Organization (WHO 2021), by the Brazilian National Environment Council (CONAMA 2018), and by the São Paulo State Environmental Council (CONSEMA 2021).

	Moving average window (hours)	*WHO standard ($\mu g.m^{-3}$)*	*BNAQ standard ($\mu g.m^{-3}$)*	*SPAQ standard ($\mu g.m^{-3}$)*
PM_{10}	24	45	120	100
O_3	8	100	140	130

Standard (BNAQ) (CONAMA 2018), the Sao Paulo State Air Quality Standard (SPAQ), and the WHO air quality guideline. Both national and state standards consist of a four-phase program, with three intermediate levels towards the WHO guideline. While the national standard is in phase 1, the state standard recently moved to its second phase, implemented in 2022 Jan 1st (CONSEMA 2021). Both the national and the state concentration levels are far less restrictive compared to the WHO guidelines.

The time series of DMMA8 and DMMA24 were correlated with each other, with correlation coefficients (R^2) between 0.68 and 0.87. A unique time series representing the average conditions in the MASP was obtained by calculating the mean time series, considering the ten monitoring stations. The annual means of DMMA8 and DMMA24 were also calculated with the aim of investigating long-term trends. Trend lines were fitted to the annual averages, obtaining the slope value for each station. The significance of the long-term trends was evaluated using the Mann-Kendall test. The null hypothesis of the Mann-Kendall test is the absence of a monotonic trend. p-values smaller than 0.05 indicate a significant trend, considering a statistical significance of 95%.

The package "fitdistrplus" from the software R was used to fit different models of PDF to the daily time series of PM_{10} and O_3 concentrations, based on the maximum log likelihood. Empirical and theoretical PDFs, as well as their parameters and cumulative distribution function (CDF) plots, were obtained for each pollutant. Complementary cumulative distribution function (CCDF) plots, defined as 1 - CDF, were calculated to retrieve the probability of exceeding the air quality standards.

Six models of probability distribution were tested: Normal, Lognormal, Gamma, Weibull, Gumbel, and Pearson V. The equation for each PDF model is shown in Table 3, as well as the respective equations for the expected value ($E[x]$), and variance ($\sigma^2[x]$). Three time periods were considered and intercompared: the whole study period (2000-2023), three recent years (2021-2023), and the year 2020, when mobility restrictions due to the COVID-19 pandemic affected air pollution concentrations in the MASP (NAKADA & URBAN 2020, RUDKE et al. 2021).

2.2 Goodness of fit

The PDF model that was better suited for the empirical data was chosen based on the Kolmogorov-Sminirnov (KS) and on the Anderson-Darling (AD) statistics, as well as in the root mean square error (RMSE) of residuals. The package "goftest" from the software R was used to calculate these metrics. KS and AD were not used as statistical tests per se but as a qualitative indication of compatibility between the sample

TABLE 3 – Definition of probability density functions (PDF) for a continuous variable x, representing air pollutant concentrations. Expected values (means) and variances are also shown based on the PDF's parameters. Adapted from WILKS (2011).

Model	*PDF Equation*	*Expected value*	*Variance*
Normal	$f(x) = \frac{1}{\sigma\sqrt{2\pi}} e^{-\frac{1}{2}\left(\frac{x-\mu}{\sigma}\right)^2}$	μ	σ^2
Lognormal	$f(x) = \frac{1}{x\,\sigma_g\sqrt{2\pi}} e^{-\frac{1}{2}\left(\frac{lnx-\mu_g}{\sigma_g}\right)^2}$	$exp[\mu_g + \frac{{\sigma_g}^2}{2}]$	$(e^{{\sigma_g}^2} - 1).\, e^{2\mu_g + {\sigma_g}^2}$
Gamma	$f(x) = \frac{\beta^\alpha}{\Gamma(\alpha)} x^{\alpha-1} e^{-\beta x}$	$\frac{\alpha}{\beta}$	$\frac{\alpha}{\beta^2}$
Weibull	$f(x) = \frac{k}{\lambda}\left(\frac{x}{\lambda}\right)^{k-1} e^{-\left(\frac{x}{\lambda}\right)^k}$ $(x, k, \lambda > 0)$	$\lambda\Gamma(1 + \frac{1}{k})$	$\lambda^2(\Gamma(1 + \frac{2}{k}) - \Gamma^2(1 + \frac{1}{k}))$
Gumbel	$f(x) = \frac{k}{\lambda}\left(\frac{x}{\lambda}\right)^{k-1} e^{-\left(\frac{x}{\lambda}\right)^k}$ $(x, k, \lambda > 0)$	$\mu + \gamma\beta$ (γ is the Euler-Mascheroni constant)	$\frac{\beta\pi}{\sqrt{6}}$
Pearson V	$f(x) = \frac{\beta^\alpha}{\Gamma(\alpha)} x^{-\alpha-1} e^{-\frac{\beta}{x}}$	$\frac{\beta}{\alpha - 1}$	$\frac{\beta^2}{(\alpha-1)^2(\alpha-2)}$

and the fitted PDF model. The smaller the KS and AD values, the better the model is adjusted to the dataset. This procedure has been adopted in the literature (MIJIĆ et al. 2009, SHARMA et al. 2016).

The one-sample KS nonparametric statistical test is based on the maximum difference (D) between the empirical cumulative distribution function (ECDF) and the modeled cumulative distribution function (CDF) (BONAMENTE 2017). The smaller the value of this distance, the better the model fits the empirical probability distribution. The KS value is more sensible when assessing the goodness of fit in the central part of the distributions. The Anderson-Darling (AD) statistical test is a modified version of the KS statistical test (LAIO 2004), also used as a goodness of fit criteria to decide between different PDF models. The AD test is more sensible for assessing the goodness of fit in the distribution extremes.

3 RESULTS AND DISCUSSION

3.1 Long-term trends and seasonal variability

Figure 2a shows the annual means of PM_{10} DMMA24 concentrations, considering all data separated by season. On average, there was a decrease of 1.04±0.09 $\mu g.m^{-3}.year^{-1}$ in the MASP PM_{10} concentrations, with more intense negative trends in the winter and fall. The PM_{10} decreasing trends were statistically significant for all seasons, according to the Mann-Kendall test (Table 4). When analyzed separately, all monitoring stations showed a significant decreasing trend in PM_{10} concentrations, although with different intensities (Supplementary Material, Table S1). Previous reports for MASP showed PM_{10} decreasing trends in the period 1996-2009 in the range of 0.78 to 3.46 $\mu g.m^{-3}.year^{-1}$, depending on the monitoring station (CARVALHO et al. 2015). Our results demonstrate that the decreasing trend of PM_{10} concentrations persisted until 2023, although the slopes have diminished, on average, when considering a group of stations representative of the whole MASP. The decrease in PM_{10} concentrations is likely associated with public policies concerning vehicular and industrial air pollution emission control, which have been progressively implemented since the 1980s in Brazil (CARVALHO et al. 2015, ANDRADE et al. 2017). Long-term decreases in PM_{10} concentrations have also been observed in other cities worldwide, like in India (GURJAR et al. 2008, ZHANG et al. 2017) and in South America (GÓMEZ PELÁEZ et al. 2020).

The O_3 long-term trends were less clear compared to PM_{10}, although positive trends were statistically significative when considering the whole year and the summer (Figure 2b and Table 4). This result indicates that the adopted policies on air pollution emission control were not effective

TABLE 4 – Trends in PM_{10} (DMMA24) and O_3 (DMMA8) concentrations between 2000 and 2023, considering data from the whole year and for each season separately. Uncertainties are represented in parenthesis. Trends statistically significant ($p<0.05$) were highlighted in italic.

		All data	*Summer*	*Fall*	*Winter*	*Spring*
PM_{10}	Slope ($\mu g.m^{-3}.yr^{-1}$)	*-1.04(9)*	*-0.78(9)*	*-1.01(11)*	*-1.48(16)*	*-0.87(15)*
	p-value	$<10^{-6}$	$<10^{-5}$	$<10^{-5}$	$<10^{-6}$	$<10^{-3}$
O_3	Slope ($\mu g.m^{-3}.yr^{-1}$)	*0.30(13)*	*0.51(22)*	0.28(19)	0.20(16)	0.23(26)
	p-value	0.018	0.04	0.33	0.19	0.33

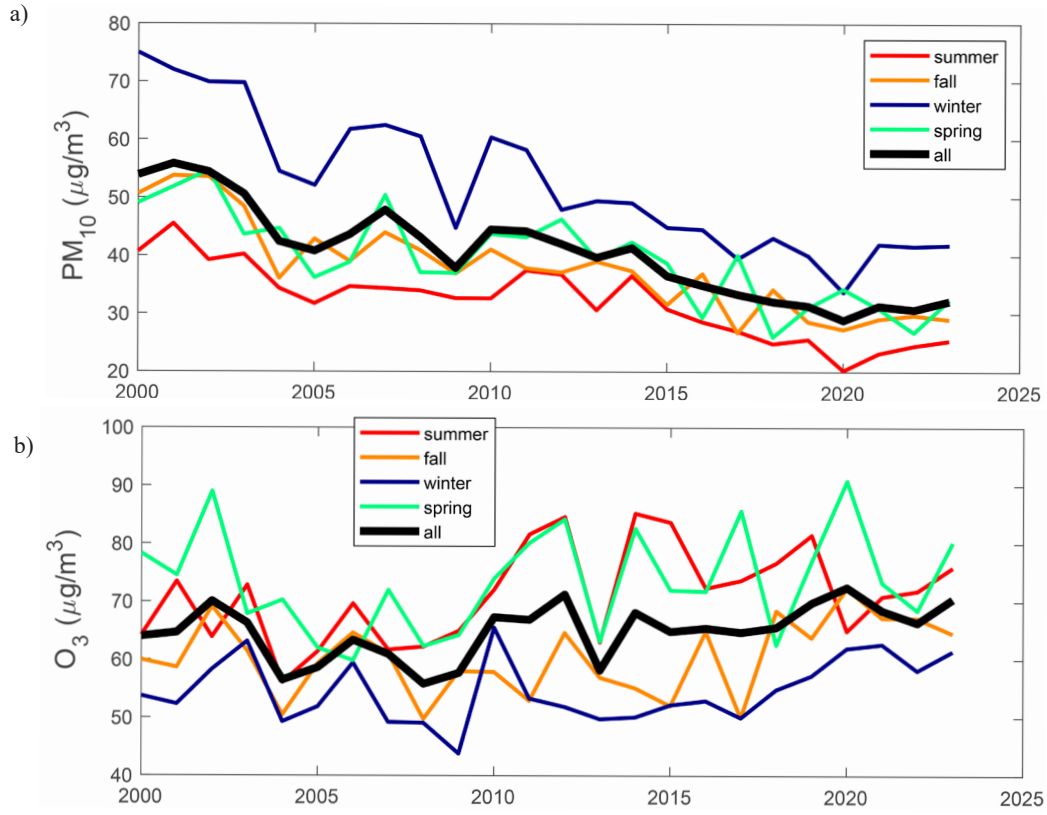

FIGURE 2 – Annual means of PM_{10}-DMMA24 (a) and O_3-DMMA8 (b) concentrations in the MASP between 2000 and 2023.

in reducing O_3 concentrations. For a complete understanding of the reasons behind the variability of the O_3 trends in different seasons, analysis of radiation, cloud cover, VOCs concentration, and speciation would be required, which is beyond the scope of the current study. In the MASP and other urban areas, tropospheric O_3 production typically increases with VOCs and decreases with NOx concentrations, under a VOC-limited production regime (ALVIM et al. 2017). The main NOx sources in the MASP are the heavy-duty vehicles (CETESB 2023), which have been subjected to emission controls resulting in a long-term decrease in NOx concentrations, similar to PM_{10}. In addition to the decreasing trends in NOx concentrations (CARVALHO et al. 2015), the interannual variation of O_3 also responds to changes in the emission patterns of hydrocarbons and in weather conditions since it is produced photochemically in the atmosphere. According to SANTOLAYA et al. (2019), weather and chemical forcing have a similar magnitude driving the O_3 interannual variability in the MASP. Other studies have shown that changes in the relative proportion of ethanol and gasoline fuel sales impacted the hydrocarbon emission patterns and the O_3 concentrations in the MASP (SALVO & GEIGER 2014, SCHUCH et al. 2019). The absence of a clear trend in O_3

concentrations is very common in urban areas (PARRISH et al. 2011, ZHANG et al. 2017, GÓMEZ PELÁEZ et al. 2020). The city of Los Angeles (USA) is a notable exception, showing a significant fall in O_3 and precursor concentrations in 50 years due to effective public policies for the control of secondary air pollutants (POLLACK et al. 2013).

When analyzing the seasonal variability of PM_{10} and O_3, as depicted in figure 3, it becomes evident that there is an increase in PM_{10} during the austral winter. Regarding O_3, the increase in concentrations occurs between September and February, corresponding to the austral spring and summer. This pattern of PM_{10} increase during the winter is associated with the enhanced atmospheric stability and dry conditions, typically observed in the MASP during the winter, hindering the dispersion of this pollutant (CARVALHO et al. 2015, OLIVEIRA et al. 2022). On the other hand, O_3, being a secondary pollutant formed by photochemical processes, increases during the spring and summer due to the higher temperatures and larger input of solar energy, favoring O_3 formation in the troposphere (SCHUCH et al. 2019).

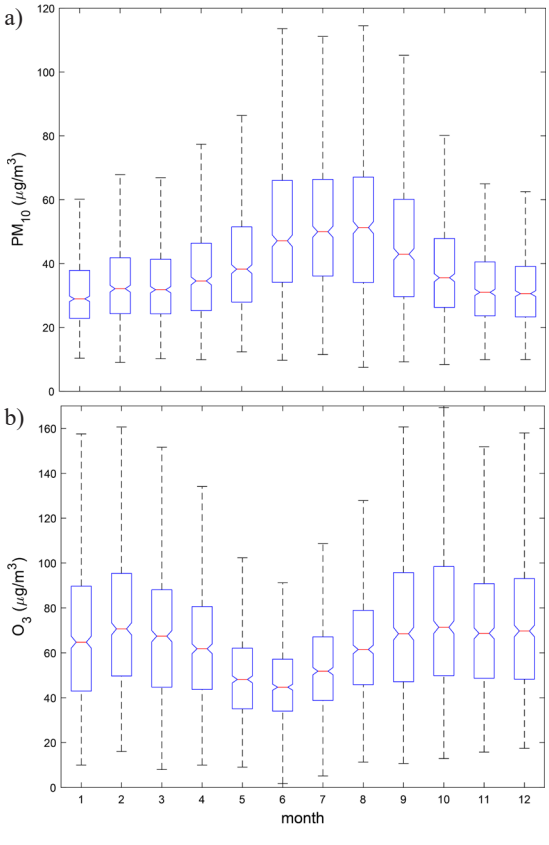

FIGURE 3 – Seasonal variability of PM_{10}-DMMA24 (a) and O_3-DMMA8 (b) concentrations in the MASP between 2000 and 2023.

3.2 Probability Distribution Functions (PDF) of PM_{10} and O_3 concentrations

The probability distribution of PM_{10}-DMMA24 and O_3-DMMA8 relies on anthropic and environmental factors that influence the atmospheric concentrations of these pollutants. Six PDF models were fitted to the PM_{10} and O_3 time series. Figure 4 shows the histogram of PM_{10} and O_3 concentrations and the fitted PDFs. The best PDF model in each case was chosen considering the lowest values obtained for the metrics KS, AD, and RMSE in a comparative way. The lowest KS

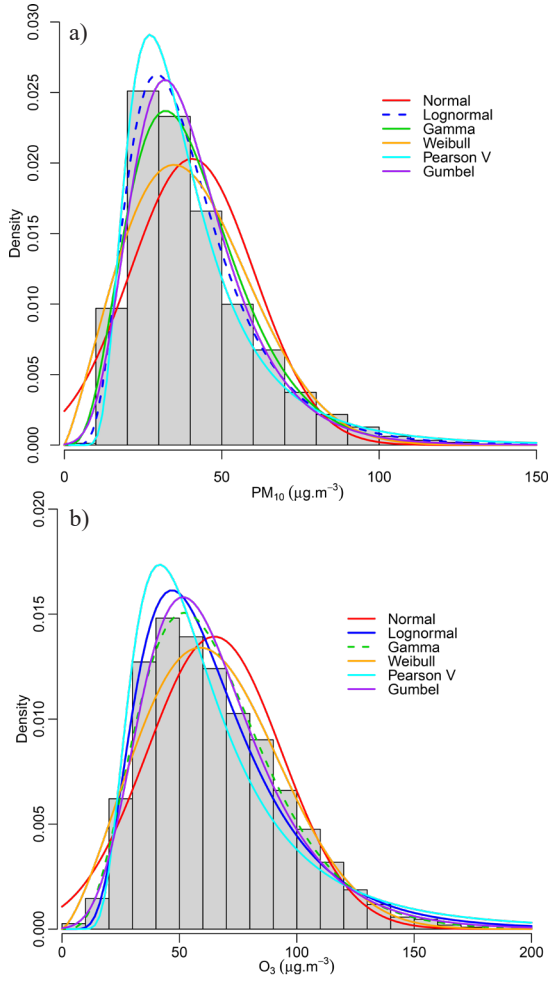

FIGURE 4 – Relative frequency histograms of PM_{10} (a) and O_3 (b) concentrations and the corresponding probability density functions (PDF) fitted to the data. Density is adimensional. The best PDF model in each case was highlighted by dashed lines.

and AD values in each case were highlighted in italic in table 5.

TABLE 5 – Goodness of fitting metrics for the different types of probability density functions adjusted to PM_{10} and O_3 concentrations: Kolmogorov-Sminirnov (KS), Anderson-Darling (AD), and root mean square error (RMSE). Values in italic highlight the smallest metrics in each case, indicating qualitatively that the model is suited to represent the distribution of concentrations.

	PM_{10}			*O_3*		
	KS	*AD*	*RMSE*	*KS*	*AD*	*RMSE*
Normal	0.095	187	35.10^{-4}	0.06	79	18.10^{-4}
Lognormal	*0.015*	*3*	*5.10^{-4}*	*0.03*	*19*	*8.10^{-4}*
Gamma	0.036	28	14.10^{-4}	*0.02*	*5*	*6.10^{-4}*
Weibull	0.063	99	26.10^{-4}	0.04	29	12.10^{-4}
Pearson V	0.030	15	10.10^{-4}	0.06	88	15.10^{-4}
Gumbel	0.034	22	13.10^{-4}	*0.03*	*9*	*8.10^{-4}*

The Lognormal was the best model for the distribution of PM_{10} concentrations. Other PDF models showed larger residuals when compared to the Lognormal model, especially for concentrations below 50 $\mu g.m^{-3}$. To our knowledge, this is the first study to characterize the probability distributions of air pollutants in the MASP. Most of the previous studies on PM_{10} in urban areas concluded that lognormal was the best model, like in Taiwan, Malaysia, and in Chinese cities (LU 2002, SANSUDDIN et al. 2011, WANG et al. 2013). Other PDF models have been applied to PM_{10}, like the Weibull and the Pearson V distribution (MIJIĆ et al. 2009, MD YUSOF et al. 2010, CREMASCO et al. 2019).

The lognormal distribution has been used to represent environmental data characterized by intrinsically positive and right-skewed values, like the growth of organisms, population dynamics, and the diffusion of radionuclides (GRÖNHOLM & ANNILA 2007). The so-called law of proportionate effect applies to variables resulting from multiplicative processes, leading to a lognormal distribution. A variable follows the law of proportionate effect if its current value is a random proportion of the previous value. The physical processes that determine PM_{10} concentrations are related to emission strengths and meteorological conditions that control PM_{10} removal and dispersion, such as wind velocity and precipitation. Previous studies indicate that the occurrence of extreme concentrations of PM_{10} in the MASP is driven by the progressive accumulation along consecutive days of unfavorable atmospheric dispersion conditions (MARTINS et al. 2017, OLIVEIRA et al. 2022), resulting in a multiplicative process. That is consistent with the law of proportionate effect and justifies the use of lognormal distributions to represent PM_{10} concentrations.

Concerning the O_3 concentrations, Gamma, Lognormal, and Gumbel PDF models were better suited to represent the observations (Table 5). The Gamma PDF model had smaller residuals compared to the others, as well as the lowest AD values, indicating a better representation of extreme values. Therefore, the Gamma model was chosen to represent the distribution of O_3 concentrations in the MASP. O_3 probability distributions are underrepresented in the literature when compared to PM_{10}. SHARMA et al. (2016) investigated the distribution of O_3-DMMA8 in Delhi, India, separating the data into four seasons. They showed that the Lognormal distribution was the best model for O_3 concentrations, except in the autumn, when the Weibull distribution was better fitted.

Table 6 shows the Lognormal and Gamma fitted parameters to PM_{10} and O_3 concentrations, respectively. The location parameters (μ_g and α) control the probability of observing moderate concentrations, while the scale parameters (σ_g and β) relate to the probability of extreme concentration values.

TABLE 6 – Parameters of Lognormal and Gamma distributions fitted to PM_{10} and O_3 concentrations in the period 2000-2023.

		Parameters
Lognormal PDF	μ_g	3.596 ± 0.005
PM_{10}	σ_g	0.463 ± 0.003
Gamma PDF	α	5.01 ± 0.07
O_3	β	0.0772 ± 0.0012

3.3 Probability of Exceeding Air Quality Standards

Using PM_{10}-DMMA24 and O_3-DMMA8 data and having defined the PDF model for each pollutant, CCDF plots were built to retrieve the probability of exceeding a certain concentration level. Three different periods were compared: the whole study period (2000-2023), the last three years (2021-2023), and the year 2020, when mobility

restrictions due to the COVID-19 pandemic affected the air pollution emission patterns. Figure 5 shows the CCDF curves for PM_{10} and O_3, and table 7 compares the probability (P) of exceedance of different air quality standards (WHO, BNAQ, and SPAQ, Table 2) in different periods of time.

The probability of observing PM_{10} concentrations above 45 $\mu g.m^{-3}$ (WHO guideline) decreased from 32.7% in the period 2000-2023 to 17.4% in recent years (2021-2023). That corroborates the long-term trends observed for PM_{10} (Fig. 2). Despite the relevant improvement, a 17.4% frequency of PM_{10} exceedance days is still unacceptably high, corresponding to 63 days of poor air quality conditions per year. Concerning O_3, regardless of the increasing trends in the mean concentrations, a decrease in the data dispersion was observed, so the probability of O_3 exceedances of the WHO guideline also decreased when comparing the whole study period (12.3%) and the last three years (11.0%). That can be partially explained by the increased variability of atmospheric conditions throughout the study period, which favors the probability of extreme concentration values for O_3. Even so, an exceedance probability of 11% corresponds to 40 days per year of harmful O_3 concentrations, according to the WHO guideline.

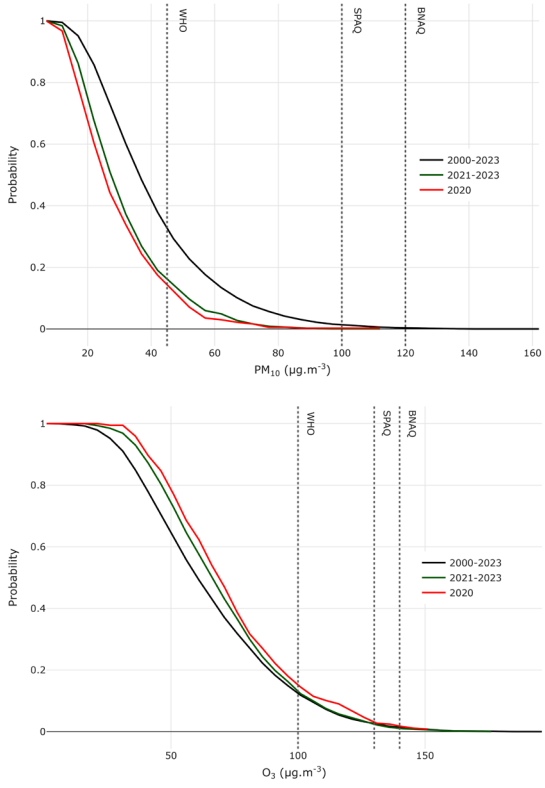

FIGURE 5 – Complementary empirical cumulative distribution functions (CCDF) depicting the probability of exceeding a certain concentration level for (a) PM_{10} and (b) O_3, considering the periods 2000-2023, 2021-2023, and 2020. Vertical lines represent the WHO, BNAQ, and SPAQ air quality standards.

This outstanding frequency of exceedance on PM_{10} and O_3 concentrations has substantial consequences for human health. If the WHO guideline for PM_{10} was met, 1500 cardiovascular and respiratory hospitalizations could be avoided annually in Sao Paulo, according to ABE & MIRAGLIA (2016). The same study showed that compliance with the WHO standard of O_3 could avoid more than 50 respiratory hospitalizations annually and postpone 152 deaths. It is important to highlight that the frequency of exceedance is not captured by the national and subnational air quality standards because they are laxer compared to the WHO guidelines. Brazilian air quality standards should move forward, reducing concentration limits according to the WHO guidelines, which have been proven to be safe for human health.

On one side, when compared to Asian cities, the exceedance probabilities in the MASP are significantly lower. Considering the PM_{10} standard of 150 $\mu g/m^3$, the literature reports probabilities of exceedance ranging from 0.5 to 7.9% in Malaysian and Chinese cities (LU 2002, MD YUSOF et al. 2010), while this probability was below 0.1% in the MASP. In the case of O_3, SHARMA et al. (2016) showed an exceedance probability of 17% for the city of Delhi, India. Compared to our results, it is possible to say that air quality conditions in MASP are significantly better concerning PM_{10} and O_3 concentrations. On the other hand,

TABLE 7 – Expected values (E), standard deviation (σ), and probability (P) of exceeding air quality standards, considering three different periods: 2000-2023, 2021-2023, and 2020.

PM_{10}			
Period	*2000-2023*	*2021-2023*	*2020*
E[x] ±σ[x] ($\mu g.m^{-3}$)	41 ± 20	31 ± 15	29 ± 14
P>45 $\mu g.m^{-3}$ (%)	32.7	17.4	15.0
P>100 $\mu g.m^{-3}$ (%)	1.3	<0.1	0.3
P>120 $\mu g.m^{-3}$ (%)	0.3	<0.1	<0.1
O_3			
Period	*2000-2023*	*2021-2023*	*2020*
E[x] ±σ[x] ($\mu g.m^{-3}$)	65 ± 29	68 ± 25	73 ± 26
P>100 $\mu g.m^{-3}$ (%)	12.3	11.0	14.5
P>130 $\mu g.m^{-3}$ (%)	2.5	1.6	3.0
P>140 $\mu g.m^{-3}$ (%)	1.4	0.5	1.6

MASP probabilities are higher than European directives (EUROPEAN COUNCIL 2008), which recommends a maximum of 35 days per year (i.e., 9.5%) with PM_{10} concentrations above 35 $\mu g.m^{-3}$. In other words, the situation has improved, but there is plenty of room to make more progress toward better air quality conditions at the MASP.

In 2020, there was a 6% decrease in PM_{10} and a 7% increase in O_3 expected values compared to the 2021-2023 period, both statistically significant according to the Mann-Whitney U Test ($p<0.01$ and $p = 0.02$, respectively). Changes in PM_{10} and O_3 concentrations can be partially explained by changes in air pollution emission patterns associated with restrictions to economic production and mobility in the first months of the COVID-19 pandemic. Weather conditions may also have influenced air pollutant concentrations in 2020, especially precipitation, which is an important atmospheric removal process for PM_{10}. The rainy season was abnormal in 2020, with precipitation above the average before the pandemic (February) and below the average in the months of most severe mobility restrictions (March to June) (RUDKE et al. 2021). When analyzing the PDF of air quality stations separately (Supplementary Material, Table S2 and S3), the PM_{10} concentration decrease in 2020 was stronger in stations influenced by industrial activities like Capuava and Mauá. Accordingly, official data about industrial production in the São Paulo state registered a 25% fall in the second trimester of 2020 compared to the previous year (IBGE 2022). Concerning O_3, there was a significant increase in the expected values and in the probability of exceedances in 2020, likely related to the decrease in NOx vehicular emissions reducing the O_3 titration in a VOC-limited regime of production. Changes in O_3 concentration during the pandemic have been reported in other cities around the world (SICARD et al. 2020, HUANG et al. 2021). Previous studies about the impact of the COVID-19 pandemics on air quality in São Paulo corroborated our results, showing a decrease in PM_{10} concentrations and an increase in O_3 concentrations, especially at the beginning of the mobility restrictions (NAKADA & URBAN 2020, RUDKE et al. 2021).

4 CONCLUSION

The statistical behavior of PM_{10} and O_3 concentrations in the period 2000-2023 was analyzed in the MASP. PM_{10} concentrations followed lognormal probability density functions, with expected values in the range of 31 ± 15 $\mu g/m^3$ (daily maximum of 24h moving averages) in recent years. PM_{10} concentrations showed a consistent long-term trend of -1.04 ± 0.09 $\mu g/m^3$/year, within the 99% significance level. Despite the long-term air quality improvement in the MASP, the probability of exceedance of the WHO guidelines was 17.4% for PM_{10} in recent years (2021-2023).

Concerning O_3, its concentration followed the Gamma probability density function, with an expected value of 68 ± 25 $\mu g/m^3$ (daily maximum of 8h moving averages) in recent years (2021-2023). Unlike PM_{10}, a positive long-term trend in O_3 was observed in the MASP, especially in the summer, when the concentrations are typically higher. It indicates that O_3 control requires distinct mitigation strategies in the MASP, accounting for the non-linear dependency of O_3 photochemical production on precursor concentrations. The frequency of WHO standard exceedance for O_3 was smaller (11%) compared to PM_{10}.

Although there have been improvements in the MASP air quality in the last 20 years, the number of days with concentrations above the WHO guidelines is still relatively high, respectively 63 and 40 days per year for PM_{10} and O_3. That imposes serious risks to the population's health, given the undisputed relationship between air pollution exposure and respiratory-cardiovascular diseases. Noteworthy, considering the lenient national and state air quality guidelines, the frequency of exceedances is typically below six days per year. To improve air quality management in the MASP and other Brazilian cities, the results from this study support the need to advance Brazilian air quality standards in accordance with WHO guidelines. Restrictive measures on vehicular and industrial emissions may be considered, particularly in periods with weather conditions unfavorable to air pollution dispersion.

In the pandemic year of 2020, there was a shift in the PM_{10} distribution towards lower concentrations, with a corresponding decrease in the probability of exceedances. On the other hand, O_3 concentrations were 5% higher compared to the 2021-2023 period. Therefore, the reduction of primary emissions at the beginning of the COVID-19 pandemic was partially offset by the increase in the formation of secondary pollutants like O_3. The reduction of vehicular and industrial emissions associated with economic production and mobility restrictions in 2020 can partially

explain the changes in concentration, although the influence of weather conditions cannot be discarded.

5 ACKNOWLEDGMENTS

We thank the São Paulo state environmental agency (CETESB - Companhia Ambiental do Estado de São Paulo) for providing data on air pollutant concentrations. We thank the Brazilian National Council for Scientific and Technological Development (CNPq) for the funding (processes 405179/2021-9 and 304819/2022-0), to the reviewers for the suggestions that improved the manuscript.

6 REFERENCES

ABE, K.; MIRAGLIA, S. 2016. Health Impact Assessment of Air Pollution in São Paulo, Brazil. *International Journal of Environmental Research and Public Health*, 13(7): 694. https://doi.org/10.3390/ijerph13070694

ALVIM, D.S.; GATTI, L.V.; CORRÊA, S.M.; CHIQUETTO, J.B.; DE SOUZA ROSSATTI, C.; PRETTO, A.; SANTOS, M.H.; YAMAZAKI, A.; ORLANDO, J.P.; SANTOS, G.M. 2017. Main ozone-forming VOCs in the city of Sao Paulo: observations, modelling and impacts. *Air Quality, Atmosphere and Health*, 10(4): 421–435. https://doi.org/10.1007/s11869-016-0429-9

ANDRADE, M.F.; KUMAR, P.; DE FREITAS, E. D.; YNOUE, R.Y.; MARTINS, J.; MARTINS, L.D.; NOGUEIRA, T.; PEREZ-MARTINEZ, P.; DE MIRANDA, R.M.; ALBUQUERQUE, T.; GONÇALVES, F.L.T.; OYAMA, B.; ZHANG, Y. 2017. Air quality in the megacity of São Paulo: Evolution over the last 30 years and future perspectives. *Atmospheric Environment*, 159: 66–82. https://doi.org/10.1016/j.atmosenv.2017.03.051

BONAMENTE, M. 2017. *Statistics and Analysis of Scientific Data*. Springer, New York, 318 p.

BRITO, J.; CARBONE, S.; MONTEIRO DOS SANTOS, D.A.; DOMINUTTI, P.; DE OLIVEIRA ALVES, N.; RIZZO, L.V.; ARTAXO, P. 2018. Disentangling vehicular emission impact on urban air pollution using ethanol as a tracer. *Scientific Reports*, 8(1): 10679. http://www.nature.com/articles/s41598-018-29138-7

CAI, Y.; ZHANG, B.; KE, W.; FENG, B.; LIN, H.; XIAO, J.; ZENG, W.; LI, X.; TAO, J.; YANG, Z.; MA, W.; LIU, T. 2016. Associations of Short-Term and Long-Term Exposure to Ambient Air Pollutants With Hypertension. *Hypertension*, 68(1): 62–70. https://doi.org/10.1161/HYPERTENSIONAHA.116.07218.

CARVALHO, V.S.B.; FREITAS, E.D.; MARTINS, L.D.; MARTINS, J.A.; MAZZOLI, C.R.; ANDRADE, M.F. 2015. Air quality status and trends over the Metropolitan Area of São Paulo, Brazil as a result of emission control policies. *Environmental Science & Policy*, 47: 68–79. https://doi.org/10.1016/j.envsci.2014.11.001

CETESB. 2016. *Classificação expedita da representatividade espacial das estações de monitoramento da qualidade do ar da CETESB no Estado de São Paulo*. São Paulo, CETESB. Available at http://www.cetesb.sp.gov.br/.

CETESB. 2023. *Qualidade do ar no estado de São Paulo 2022*. São Paulo, CETESB, Série Relatórios. Available at https://cetesb.sp.gov.br/ar/wp-content/uploads/sites/28/2023/07/Relatorio-de-Qualidade-do-Ar-no-Estado-de-Sao-Paulo-2022.pdf.

CONAMA – CONSELHO NACIONAL DO MEIO AMBIENTE. 2018. *Brazilian National Environment Council, Resolution nº 491/2018*. Available at http://conama.mma.gov.br/?option=com_sisconama&task=arquivo.download&id=766.

CONSEMA – CONSELHO ESTADUAL DO MEIO AMBIENTE. 2021. *São Paulo State Environment Council, Resolution nº 04/2021*. Available at https://smastr16.blob.core.windows.net/consema/sites/15/2021/05/del-04_2021-meta-intermediaria-etapa-2-mi2.pdf.

CREMASCO, M.A.; TARANTO, O.P.; CASTILHO, G.J.; TOMAZ, E. 2019. Modelling annual data of PM10 atmospheric

in Campinas City from probability density function. *Chemical Engineering Transactions*, 74: 349–354. https://doi.org/10.3303/CET1974059.

DATAGEO. 2013. *Modelo Digital de Elevação do Estado de São Paulo*. Sistema ambiental paulista. Available at https://datageo.ambiente.sp.gov.br/. Accessed in 26 june 2024.

DOMINUTTI, P.; NOGUEIRA, T.; FORNARO, A.; BORBON, A. 2020. One decade of VOCs measurements in São Paulo megacity: Composition, variability, and emission evaluation in a biofuel usage context. *Science of the Total Environment*, 738: 139790. https://doi.org/10.1016/j.scitotenv.2020.139790.

EUROPEAN COUNCIL. 2008. *Directive 2008/50/EC of the European Parliament and of the Council of 21 May 2008 on ambient air quality and cleaner air for Europe*. Official Journal of the European Union, 1, 1–44 https://eur-lex.europa.eu/eli/dir/2008/50/2015-09-18.

GÓMEZ PELÁEZ, L.M.; SANTOS, J.M.; DE ALMEIDA ALBUQUERQUE, T.T.; REIS, N.C.; ANDREÃO, W.L.; DE FÁTIMA ANDRADE, M. 2020. Air quality status and trends over large cities in South America. *Environmental Science and Policy*, 114: 422–435. https://doi.org/10.1016/j.envsci.2020.09.009

GOUVEIA, N.; JUNGER, W.L. 2018. Effects of air pollution on infant and children respiratory mortality in four large Latin-American cities. *Environmental Pollution*, 232: 385–391. https://doi.org/10.1016/j.envpol.2017.08.125

GRÖNHOLM, T.; ANNILA, A. 2007. Natural distribution. *Mathematical Biosciences*, 210(2): 659–667. https://doi.org/10.1016/j.mbs.2007.07.004

GURJAR, B.R.; BUTLER, T.M.; LAWRENCE, M.G.; LELIEVELD, J. 2008. Evaluation of emissions and air quality in megacities. *Atmospheric Environment*, 42(7): 1593–1606. https://doi.org/10.1016/j.atmosenv.2007.10.048

HUANG, X.; DING, A.; GAO, J.; ZHENG, B.; ZHOU, D.; QI, X.; TANG, R.; WANG, J.; REN, C.; NIE, W.; CHI, X.; XU, Z.; CHEN, L.; LI, Y.; CHE, F.; PANG, N.; WANG, H.; TONG, D.; QIN, W.; HE, K. 2021. Enhanced secondary pollution offset reduction of primary emissions during COVID-19 lockdown in China. *National Science Review*, 8(2): nwaa137. https://doi.org/10.1093/nsr/nwaa137

IBGE – INSTITUTO BRASILEIRO DE GEOGRAFIA E ESTATÍSTICA. 2022. *Pesquisa Industrial Mensal - Produção Física*. Available at https://www.ibge.gov.br/estatisticas/economicas/industria/9296-pesquisa-industrial-mensal-producao-fisica-regional.html

LAIO, F. 2004. Cramer–von Mises and Anderson-Darling goodness of fit tests for extreme value distributions with unknown parameters. *Water Resources Research*, 40(9): 1-10. https://doi.org/10.1029/2004WR003204

LU, H.-C. 2002. The statistical characters of PM10 concentration in Taiwan area. *Atmospheric Environment*, 36(3): 491–502. https://doi.org/10.1016/S1352-2310(01)00245-X

MARTINS, L.D.; WIKUATS, C.F.H.; CAPUCIM, M.N.; DE ALMEIDA, D.S.; DA COSTA, S.C.; ALBUQUERQUE, T.; BARRETO CARVALHO, V.S.; DE FREITAS, E.D.; DE FÁTIMA ANDRADE, M.; MARTINS, J.A. 2017. Extreme value analysis of air pollution data and their comparison between two large urban regions of South America. *Weather and Climate Extremes*, 18: 44–54. https://doi.org/10.1016/j.wace.2017.10.004

MD YUSOF, N.F.F.; RAMLI, N.A.; YAHAYA, A.S.; SANSUDDIN, N.; GHAZALI, N.A.; AL MADHOUN, W. 2010. Monsoonal differences and probability distribution of PM10 concentration. *Environmental Monitoring and Assessment*, 163(1-4): 655–667. https://doi.org/10.1007/s10661-009-0866-0

MIJIĆ, Z.; TASIĆ, M.; RAJŠIĆ, S.; NOVAKOVIĆ, V. 2009. The statistical characters of PM10 in Belgrade area. *Atmospheric Research*, 92(4): 420–426. https://doi.org/10.1016/j.atmosres.2009.01.002

MISHRA, G.; GHOSH, K.; DWIVEDI, A.K.; KUMAR,M.;KUMAR,S.;CHINTALAPATI, S.; TRIPATHI, S.N. 2021. An application of probability density function for the analysis of PM2.5 concentration during the COVID-19 lockdown period. *Science of The Total Environment*, 782: 146681. https://doi.org/10.1016/j.scitotenv.2021.146681

NAKADA, L.Y.K.; URBAN, R.C. 2020. COVID-19 pandemic: Impacts on the air quality during the partial lockdown in São Paulo state, Brazil. *Science of The Total Environment*, 730: 139087. https://doi.org/10.1016/j.scitotenv.2020.139087

NOGUEIRA, T.; DOMINUTTI, P.A.; DE CARVALHO, L.R.F.; FORNARO, A.; ANDRADE, M.D.F. 2014. Formaldehyde and acetaldehyde measurements in urban atmosphere impacted by the use of ethanol biofuel: Metropolitan Area of Sao Paulo (MASP), 2012–2013. *Fuel*, 134: 505–513. https://doi.org/10.1016/j.fuel.2014.05.091

OLIVEIRA, M.C.Q.D.; DRUMOND, A.; RIZZO, L.V. 2022. Air pollution persistent exceedance events in the Brazilian metropolis of Sao Paulo and associated surface weather patterns. *International Journal of Environmental Science and Technology*, 19(10): 9495–9506. https://doi.org/10.1007/s13762-021-03778-1

PAPANASTASIOU, D.K.; MELAS, D. 2010. Application of PM10's statistical distribution to air quality management—A case study in Central Greece. *Water, Air, and Soil Pollution*, 207(1–4): 115–122. https://doi.org/10.1007/s11270-009-0123-8

PARRISH, D.D.; SINGH, H.B.; MOLINA, L.; MADRONICH, S. 2011. Air quality progress in North American megacities: A review. *Atmospheric Environment*, 45(39): 7015–7025. https://doi.org/10.1016/j.atmosenv.2011.09.039

PÉREZ-MARTÍNEZ, P.J.; DE FÁTIMA ANDRADE, M.; DE MIRANDA, R.M. 2017. Heavy truck restrictions and air quality implications in São Paulo, Brazil. *Journal of Environmental Management*, 202, Part 1, 55–68. https://doi.org/10.1016/j.jenvman.2017.07.022

PLOCOSTE, T.; CALIF, R.; EUPHRASIE-CLOTILDE, L.; BRUTE, F.N. 2020. The statistical behavior of PM10 events over Guadeloupean archipelago: Stationarity, modeling and extreme events. *Atmospheric Research*, 241: 104956. https://doi.org/10.1016/j.atmosres.2020.104956

POLLACK, I.B.; RYERSON, T.B.; TRAINER, M.; NEUMAN, J.A.; ROBERTS, J.M.; PARRISH, D.D. 2013. Trends in ozone, its precursors, and related secondary oxidation products in Los Angeles, California: A synthesis of measurements from 1960 to 2010. *Journal of Geophysical Research Atmospheres*, 118(11): 5893–5911. https://doi.org/10.1002/jgrd.50472

RUDKE, A.P.; MARTINS, J.A.; DE ALMEIDA, D.S.; MARTINS, L.D.; BEAL, A.; HALLAK, R.; FREITAS, E.D.; ANDRADE, M.F.; FOROUTAN, H.; BAEK, B.H.; DE, T.T. 2021. How mobility restrictions policy and atmospheric conditions impacted air quality in the State of São Paulo during the COVID-19 outbreak. *Environmental Research*, 198: 111255. https://doi.org/10.1016/j.envres.2021.111255

SALVO, A.; GEIGER, F.M. 2014. Reduction in local ozone levels in urban São Paulo due to a shift from ethanol to gasoline use. *Nature Geoscience*, 7(6): 450–458. https://doi.org/10.1038/NGEO2144

SANSUDDIN, N.; RAMLI, N.A.; YAHAYA, A.S.; YUSOF, N.F.F.M.; GHAZALI, N.A.; MADHOUN, W.A.AL. 2011. Statistical analysis of PM10 concentrations at different locations in Malaysia. *Environmental Monitoring and Assessment*, 180(1–4): 573–588. https://doi.org/10.1007/s10661-010-1806-8

SANTOLAYA, C.; OLIVEIRA, M.C.Q.D.; RIZZO, L.V.; MIRAGLIA, S.G.E.K. 2019. Contribution of chemical and meteorological factors to tropospheric ozone formation in São Paulo. *Revista Brasileira de Ciências Ambientais (Online)*, 54: 90–104. https://doi.org/10.5327/Z2176-947820190577

SANTOS, T.C.; REBOITA, M.S.; CARVALHO, V.S.B. 2018. Investigation of the relationship between atmospheric variables and the

concentration of PM10 and O3 in the state of São Paulo. *Revista Brasileira de Meteorologia*, 33(4): 631–645. https://doi.org/10.1590/0102-7786334006

SCHUCH, D.; DE FREITAS, E.D.; ESPINOSA, S.I.; MARTINS, L.D.; CARVALHO, V.S.B.; RAMIN, B.F.; SILVA, J.S.; MARTINS, J.A.; DE FATIMA ANDRADE, M. 2019. A two decades study on ozone variability and trend over the main urban areas of the São Paulo state, Brazil. *Environmental Science and Pollution Research*, 26(31): 31699–31716. https://doi.org/10.1007/s11356-019-06200-z

SHARMA, S.; SHARMA, P.; KHARE, M.; KWATRA, S. 2016. Statistical behavior of ozone in urban environment. *Sustainable Environment Research*, 26(3): 142–148. https://doi.org/10.1016/j.serj.2016.04.006

SICARD, P.; DE MARCO, A.; AGATHOKLEOUS, E.; FENG, Z.; XU, X.; PAOLETTI, E.; RODRIGUEZ, J.J.D.; CALATAYUD, V. 2020. Amplified ozone pollution in cities during the COVID-19 lockdown. *Science of The Total Environment*, 735: 139542. https://doi.org/10.1016/j.scitotenv.2020.139542

TAKANO, A.P.C.; JUSTO, L.T.; DOS SANTOS, N.V.; MARQUEZINI, M.V.; DE ANDRÉ, P.A.; DA ROCHA, F.M.M.; PASQUALUCCI, C.A.; BARROZO, L.V.; SINGER, J.M.; DE ANDRÉ, C.D.S.; SALDIVA, P.H.N.; VERAS, M.M. 2019. Pleural anthracosis as an indicator of lifetime exposure to urban air pollution: An autopsy-based study in Sao Paulo. *Environmental Research*, 173: 23–32. https://doi.org/10.1016/j.envres.2019.03.006

WANG, X.; CHEN, R.J.; CHEN, B.H. 2013. Application of statistical distribution of PM10 concentration in air quality management in 5 representative cities of China. *Biomedical and Environmental Sciences*, 26(8): 638–646. https://doi.org/10.3967/0895-3988.2013.08.002

WHO – WORLD HEALTH ORGANIZATION. 2021. *Executive summary. World Health Organization global air quality guidelines: particulate matter (PM2.5 and PM10), ozone, nitrogen dioxide, sulfur dioxide and carbon monoxide*. https://iris.who.int/handle/10665/345329

WILKS, D.S. 2011. *Statistical Methods in the Atmospheric Sciences*. Academic Press, Oxford, UK, 3rd ed.

ZHANG, Z.H.; HU, M.G.; REN, J.; ZHANG, Z.Y.; CHRISTAKOS, G.; WANG, J.F. 2017. Probabilistic assessment of high concentrations of particulate matter (PM_{10}) in Beijing, China. *Atmospheric Pollution Research*, 8(6): 1143–1150. https://doi.org/10.1016/j.apr.2017.04.006

Authors' addresses:

Matheus Soares Dário (0000-0003-3259-9137), Denise Gomes Novais (0000-0002-3285-1032) e Theotonio Pauliquevis (0000-0001-8641-3540) – Universidade Federal de São Paulo, Instituto de Ciências Ambientais, Químicas e Farmacêuticas, Rua São Nicolau, 210, CEP 0991330, Diadema, SP, Brasil. E-mails: dario@unifesp.br, denise.novais@unifesp.br, theotonio.pauliquevis@unifesp.br

Luciana Varanda Rizzo* (0000-0002-1748-6997) – Universidade de São Paulo, Instituto de Física, Rua do Matão, 1371, CEP 0991330, São Paulo, SP, Brasil. E-mail: lrizzo@usp.br

*Corresponding author

Manuscript submitted on 15 March 2024, accepted on 10 July 2024.